Electronic Supplementary Material (ESI) for Physical Chemistry Chemical Physics.

Supplemental Information for: "The Butterfly – A Well-Defined Constant-Current Topography Pattern On Si(001):H and Ge(001):H Resulting From Current-Induced Defect Fluctuations"

Mads Engelund,[*a‡] Szymon Godlewski,[b‡] Marek Kolmer,[b] Rafał Zuzak,[b] Bartosz Such,[b] Thomas Frederiksen,[c,d] Marek Szymonski,[b] and Daniel Sánchez-Portal[a,c]

[a]Centro de Física de Materiales (CFM), CSIC-UPV/EHU, Paseo Manual de Lardizabal 5, 20018, Donostia-San Sebastián, Spain.
[b]Centre for Nanometer-Scale Science and Advanced Materials (NANOSAM), Faculty of Physics, Astronomy and Applied Computer Science, Jagiellonian University, Krakow, Poland.
[c]Donostia International Physics Center (DIPC), Paseo Manual de Lardizabal 4, 20018, Donostia-San Sebastián, Spain.
[d]IKERBASQUE, Basque Foundation for Science, E-48013, Bilbao, Spain.

S1 Simple linear average is not sufficient

If we assume that the switching rate is independent on the current (corresponding to $N = 0$ in Eq. S1 below, this is the case, for example, for thermally induced switching), then the time-averaged current would be a simple average of the currents in the two configurations. As seen in Fig. S1A-B this assumption leads to quite featureless images, which cannot reproduce the experimental observations.

S2 Low sensitivity of the N parameter

Here we demonstrate that the constant-current topographies have a quite low dependence on the actual value of the order of the current dependence of the switching rates, $N \geq 1$. We use the general formula for the time-averaged current

$$\langle I(\mathbf{r})\rangle = \frac{I^N_{DB,1}(\mathbf{r})I_2(\mathbf{r}) + I_1(\mathbf{r})I^N_{DB,2}(\mathbf{r})}{I^N_{DB,1}(\mathbf{r}) + I^N_{DB,2}(\mathbf{r})}, \tag{S1}$$

and simplify the analysis by using that $I_{1(2)} \approx I_{DB,1(2)}$ close to the DBD at voltages just past the gap resonance. We note that the largest values of the time-averaged current occur at those positions where $\langle I(\mathbf{r})\rangle \approx I_1 \approx I_2$ and both are high. The lowest values of the averaged current on the other hand, occur when either I_1 or I_2 drops to a low value. Assuming $I_1 \ll I_2$ leads to $\langle I\rangle \approx 2I_1$ for $N = 1$ and $\langle I\rangle \approx I_1[1 + (I_1/I_2)^{N-1}]$ for $N > 1$. This means that the low-current state dominates the appearance for all tip positions regardless of the actual N value. Therefore, the precise value of N is not crucial for reproducing the main features of the experimental STM image. In Fig. S1 we see that, even when we let N approach infinity, the resulting topography is very similar to the $N = 1$ case. The reason for this behaviour is that for $N = 1$ the system spends most of the time in the low-current state, and as the order is increased this tendency only becomes stronger. Finally, as $N \to \infty$ the already small contribution from the high-current state is eliminated and $\langle I\rangle \approx I_1$.

It is worth to note that the analysis of the recorded STM images may provide a hint to differentiate the thermally driven from current induced switching processes. For instance the thermally driven switching should be characterized by similar occupation of both geometries irrespective of the current flowing through each configuration for a given STM tip position. This should be reflected in the STM appearance being similar to the one simulated for $N = 0$ shown in Fig. S1A-B. Therefore for switching induced by thermal excitation the STM image of the dangling-bond dimer (DBD) should be different from the one observed experimentally at low temperature. This gives further support to the current-induced switching model used in this paper. The analysis of the STM images

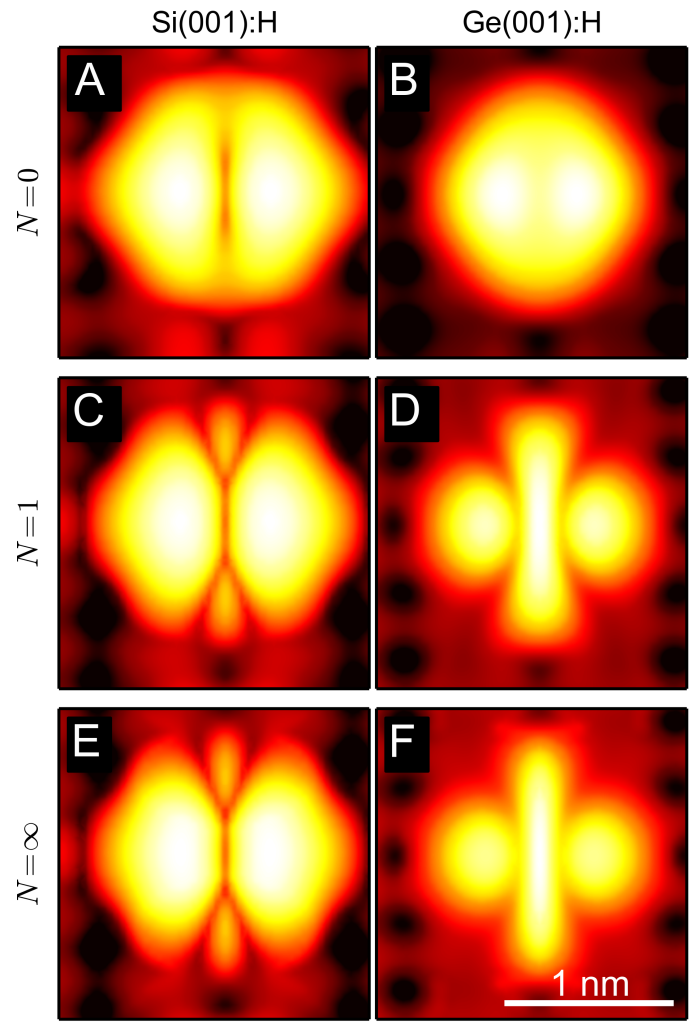

Figure S1 Simulated constant-current topographies. (A,B) correspond to a simple linear average ($N = 0$), (C,D) correspond to an assumed one-electron process ($N = 1$) as in the main text, while (E,F) are the topographies when higher-order processes dominate ($N \to \infty$).

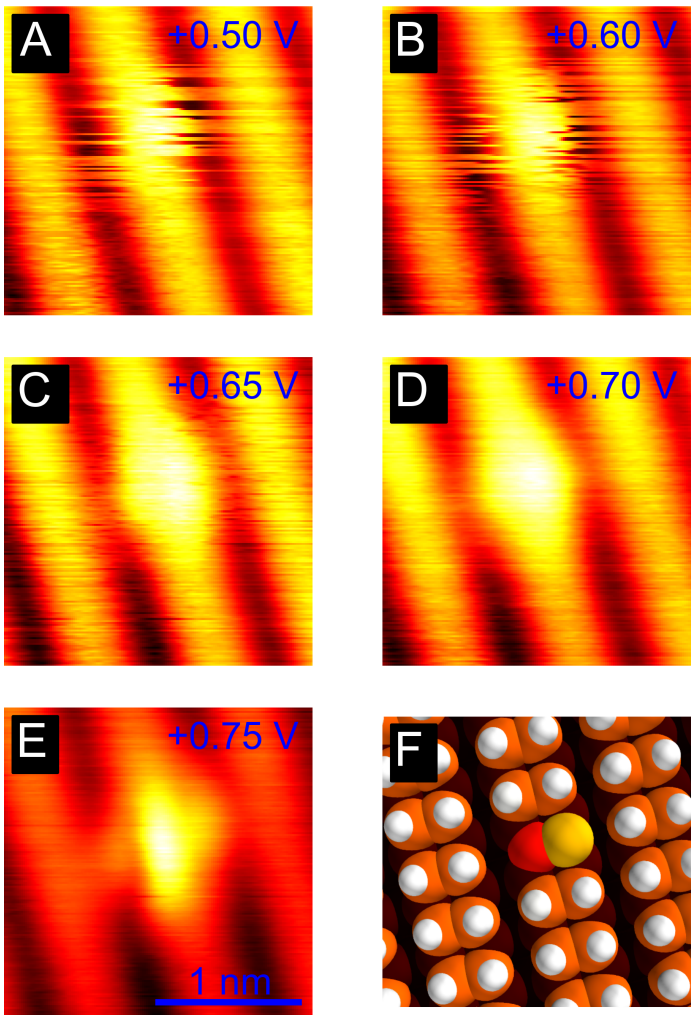

Figure S2 DBD on the Ge(001):H surface. (A-E) constant current STM images recorded with different bias voltages, all topographies recorded with $I = 10$ pA tunneling current. (F) Structural model of the imaged area, coloring identical as in Fig. S1.

of fluctuating defects could therefore also be applied to determine the driving force for switching processes, especially for defects exhibiting substantial asymmetry.

S3 Smooth appearance of the dimer at positive voltages

The rate of the DBD switching on Ge(001):H grows quickly with increased bias voltage, when the voltage reaches the tail of the recorded empty state dI/dV resonance ($V_S = 0.84$ V). This is illustrated in the series of STM images recorded with different voltages shown in Fig. S2. At lower voltages, up to $V_S = 0.6$ V single switching events are clearly discernible as demonstrated by the streaky pattern in Fig. S2A-B. However, as the voltage is further raised the switching frequency falls out of the apparatus time resolution leading to completely smooth STM topographies presented in Fig. S2C-E. Please note, that at $V_S = 0.75$ V the butterfly motif starts to be visible, with an increase of the current intensity around the center of the DBD.

S4 Reproduction of the pre-resonance behaviour

The STM model introduced in the main text is applicable both at voltages below and above the resonance. Below the resonance there is an additional complication - the current into the DBD unoccupied resonance is no longer the dominant contribution to the overall current, i.e., using the nomenclature of the main text $I_{DBD,1(2)} \ll I_{O,1(2)}$, but remains (by assumption) the unique cause of switching events. Due to the *de facto* p-doping of the Ge(001):H substrate, we assume that the Fermi level is at the valence band and we use a 0.1 eV (gaussian) state broadening which both broadens the DBD resonance and creates a current contribution from the top of the valence band (I_{VB}), which below the DBD resonance, has the dominant contribution to the total current ($I_T = I_{VB} + I_{DBD}$). As observed in Fig. S3, it is possible to reproduce the features of current-topographies for the smooth STM images (see Fig. S2C) which occur before the appearance of the butterfly motif. We note that the precise choice of the Fermi level and state broadening does not influence the qualitative result.

The central determining factor in the overall shape of the simulated topography before resonance (Fig. S3) is that the configurations giving the highest I_{DBD} contribution and the highest total current I_T is reversed in the vicinity of the DBD. Let us for a voltage below the DBD resonance, and for a specific point, denote the state giving the highest and lowest total STM current as 'H' and 'L', respectively. We have $I_{T,H}/I_{T,L} \approx I_{VB,H}/I_{VB,L} > 1$, while $I_{DBD,H}/I_{DBD,L} < 1$, meaning that the current through the DBD resonance is higher in the state giving the lowest overall current (L).

Since the switching of the dimer is, according to our model, only determined by the fraction of the current flowing through the DBD resonance, I_{DBD}, then for voltages below the DBD resonance the system spends a longer time in the high-total-current state H. The fraction of time spent in the H configuration is $n_H = 1/[1 + (I_{DBD,H}/I_{DBD,L})^N] > 1/2$. So in this regime the state giving the highest total current I_T dominates the topography, as it has both the highest current and the highest occupation. As a result we see a uniformly high current near the DBD.

At low voltages, before the image becomes smooth, the model still makes predictions about the relative time spent in the two states, $n_{1(2)}(\mathbf{r})$, although it makes no prediction of the absolute switching rate. According to our model, the system will spend the majority of the time in the high-total-current state H and as seen in Fig. S4 this higher occupation of the high-current state is indeed observed for low positive-voltage current trace. Note that the precise current value at a specific point is highly sensitive to the uncertainty in the STM modeling – in contrast to the overall features of topographic images. We therefore limit ourselves to this general observation.

In general, the experimental observations of the pre-resonance regime is fully consistent with our two-level model when the exitence of two different contributions to the tunneling current is recognized (one causing switching, and the other not).

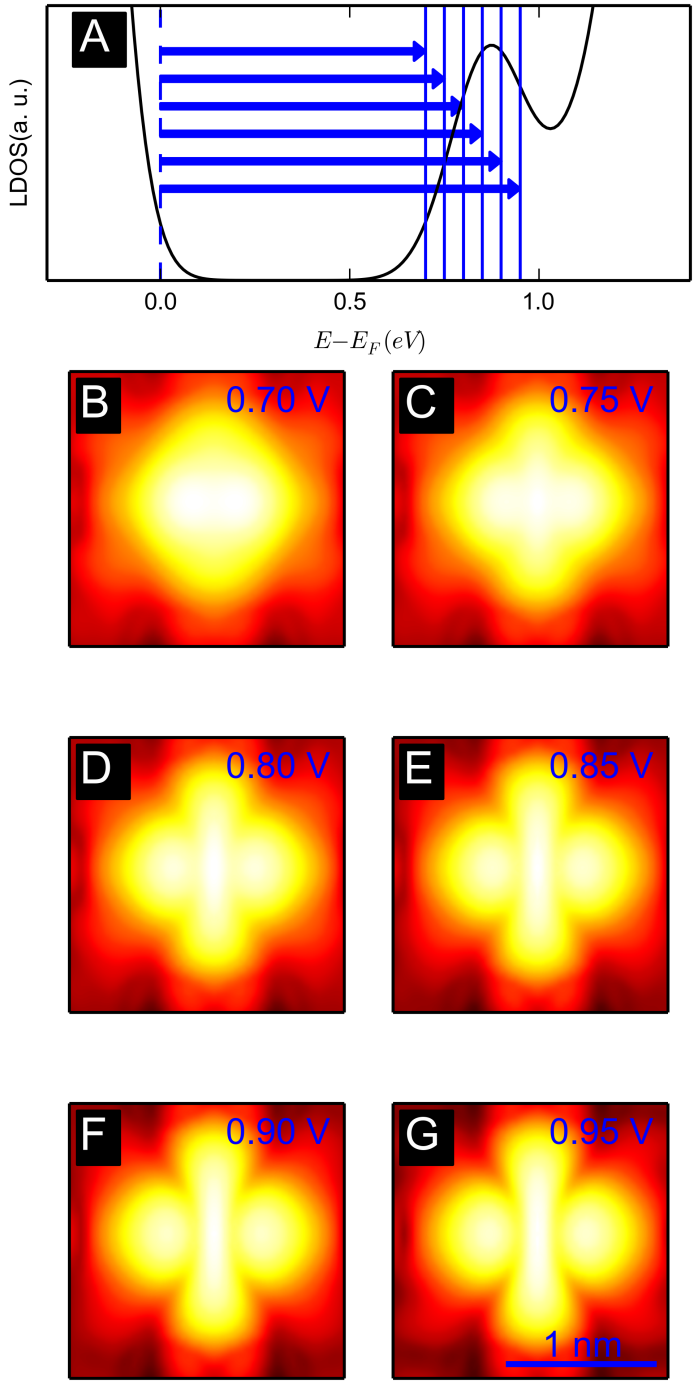

Figure S3 (A) Local density of states directly above the Ge DBD (8 Å above the plane defined by the hydrogen atoms that saturate the other Ge dimers on the surface). The blue arrows and vertical lines show the bias windows used to simulate the current-topographies (B-G) as a larger and larger part of the DBD resonance is swept.

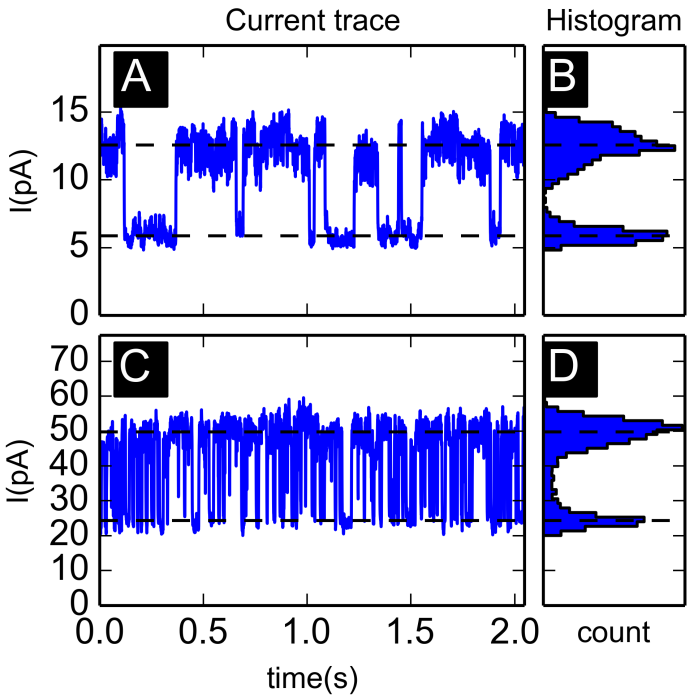

Figure S4 (A,C) Current time traces and (B,D) corresponding current histograms for two different tip-sample separations and a sample bias V_S=0.45 V. The observed current values separate into two distinct levels and the highest current level is observed most frequently, which is consistent with the theoretical observation that for positive bias voltages well below the DBD resonance the total tunneling current is dominated by other contributions different from the current flowing through the DBD resonance that causes the switching.